

Novel Z-Chart for Predicting Insufficient Oil of Automotive Belt-Driven Air Conditioning Compressor

Muhammad Nur Othman^{a,b}, Mohd Zaki Nuawi^{a*}, Nor Azazi Ngatiman^b & Muhammad Yuszairie Yusri^b

^a*Department of Mechanical and Manufacturing Engineering, Faculty of Engineering & Built Environment, Universiti Kebangsaan Malaysia, Malaysia.*

^b*Department of Engineering Technology, Faculty of Mechanical Technology and Engineering, Universiti Teknikal Malaysia Melaka, Malaysia.*

*Corresponding author: mzn@ukm.edu.my

Received 30 July 2024, Received in revised form 18 March 2025

Accepted 22 April 2025, Available online 30 July 2025

ABSTRACT

Automotive air conditioning systems play a vital role in ensuring comfort and safety, particularly in tropical climates where high temperatures and humidity demand reliable cooling. The compressor, as the main component, is essential for circulating refrigerant and maintaining system efficiency. Ensuring the compressor operates is crucial as it compromises the performance and could impact the overall functionality of the air conditioning system. The moving components inside the compressor, such as the bearing and piston, require lubrication with a specific quantity of oil. Therefore, maintaining optimal compressor oil levels is crucial to prevent system inefficiencies and potential mechanical failures. This study introduces a novel diagnostic approach using Z-freq 3D statistical analysis to monitor and predict insufficient or excessive oil levels in belt-driven air conditioning compressors. Triaxial vibration data were collected using wireless accelerometers across varying compressor speeds and oil quantities. The data were analyzed and formed into a novel Z-Chart, a control chart that correlates vibration characteristics with oil adequacy. Results reveal that compressors with 80 ml of oil exhibited the lowest vibration, while both insufficient (40 ml, 60 ml) and excessive (100 ml, 120 ml) oil levels led to higher vibration due to suboptimal performance. The Z-Chart, based on the 'b/a' coefficient derived from the Gauss Amp model, provides a new visual and quantitative tool for predictive maintenance, enabling early detection of oil-related issues. This method offers significant implications for the automotive industry by reducing operational costs and enhancing compressor reliability. Future research could integrate this technique with IoT-enabled real-time monitoring systems to further improve maintenance practices.

Keywords: Z-chart analysis; compressor oil diagnosis; vibration monitoring; predictive maintenance; automotive air conditioning compressor

INTRODUCTION

Air conditioning (AC) has become indispensable for all vehicles, irrespective of whether they operate in urban or rural environments. Currently, the weather has intensified in heat as a result of global climate change (Duan et al. 2023; Harvey, Bain-Donohue & Dewi 2024; Randazzo, Pavanello & De Cian 2023). Moreover, the increase in temperature has resulted in fatalities. K. Fakagawa et al. (2023) documented 805 fatalities in 2022 attributable to heat stroke. Nonetheless, the continuous operation of air conditioning significantly elevates a vehicle's energy

consumption, as it constitutes a substantial auxiliary energy drain, accounting for 75.9% of total brake horsepower or 9.97 kW out of a total of 13.13 kW at 3000 rpm (Gajanayake, Bandara & Sugathapala 2023). Despite its significant energy consumption, the AC system is installed in all new automobiles on the market due to its essential nature.

Automotive Air Conditioning (AAC) systems facilitate a cool and comfortable cabin atmosphere, enhancing driver comfort, particularly during hot weather and extended driving periods (Chen et al. 2020). It also aids in maintaining optimal visibility of the windscreen and windows under humid driving conditions, where

misting may commonly arise (Fan et al. 2022). Poor maintenance of the air conditioning system may result in elevated cabin temperatures, thereby causing driver tiredness and diminished focus (Vasta 2023). Health conditions also could be affected by poor air quality due to dirty air filters that collect dust, pollen and airborne particles that are not properly maintained (Golofit-Szymczak, Stobnicka-Kupiec & Gorny 2019). Maintaining an AAC system is essential for establishing a comfortable, safe, and healthy environment within the cabin.

AAC systems have evolved from basic cooling apparatuses to intricate machines that incorporate advanced technologies over the past few decades. AAC systems operate by altering a refrigerant's properties to extract heat from the cabin and expel it externally. The fundamental refrigerant cycle is propelled by four primary components: a compressor, a condenser, an expansion valve, and an evaporator. Consequently, the majority of the research concentrates on the four primary components, the controller and the refrigerant, serving as a medium. Recent investigations into refrigerants such as R1234yf, R513A, and CO₂, in comparison to R134A, aimed to develop an eco-friendly, more efficient, and higher-performing refrigerant (Al-Zahrani 2024; Patel & Parekh 2024; Saadoon & Aljubury 2019). S. Shalgar et al. (2022) engineered the incorporation of intelligent sensors inside a multichannel data acquisition system for the continuous monitoring of temperature, pressure, and humidity in a hybrid ACC. The performance of AAC may be effectively monitored using several forms of data mapping. T. Parent et al. (2023) examined on the controller side, a nonlinear modeling control system for the compressor, condenser fan, front-end underhood airflow, and active grille shutter position. Similar work was also carried out by S. Schaut et al. (2020), who conducted analogous research, proposing linear quadratic model predictive control algorithms for managing heat conditions in battery compartments while accounting for passenger comfort. The most recent work on the compressor was done to improve the performance and efficiency of the compressor by Z. Li et al. (2024), who studied variable displacement compressors versus variable speed compressors integrated with a heat pump system. Nevertheless, advanced materials, including diamond-like carbon film coating technology, were employed for the scroll-type compressor of AAC (He, Ji & Xing 2020). Despite evaluating performance, efficiency, and environmental sustainability in automobile air conditioning, predictive maintenance and condition monitoring are crucial for prolonging the system's lifespan (Sanzana et al. 2022).

The core component of an AAC is the compressor, which compresses the refrigerant gas and elevates its temperature. The high-temperature, high-pressure

refrigerant gas then flows to the condenser, which is cooled by the outside air that moves through the condenser fins with the help of the condenser fan and transforms the refrigerant state from a gas into a liquid. Before entering the evaporator, this liquid refrigerant goes through the expansion valve, which reduces its temperature and pressure and converts its condition to moisture. The cold refrigerant then absorbs heat from the car's interior in the evaporator with the help of a blower to circulate the cabin air. The process thereafter returns to the compressor to initiate the cycle anew. There are two types of compressors now utilized by automobiles, which are belt-driven compressors which is driven by the car's engine powers through the belt and electric-driven compressor, which drive electric power from the car's battery (Zawawi et al. 2024). Substantial interest and body of literature exist on novel nano lubricant oils for compressors, as evidenced by the works of researchers such as Safril et al. (2024), A. Alahmer et al. (2023), A. Hamisa et al. (2023) and N. Zawawi et al. (2023). H. Zang et al. (2022) attempted condition monitoring of gear-bearing in a centrifugal compressor via self-excitation of vibration. Similar work has also been pursued by S. Kumar et al. (2024) have also conducted analogous research on the condition monitoring of gears in an electric vehicle motor. M. Satar et al. (2021) conducted a laboratory-scale experiment to plot and compare the hissing noise generated by AAC components, including the TVX, evaporator, and compressor. Other researchers endeavor to mitigate the humming noise from ACC by implementing a tunable dynamic vibration absorber (Aziz et al. 2022). Numerous studies have examined compressor vibration, primarily focusing on residential and industrial units, including vibration dampers by W. Xiao et al. (2023), acoustic enclosures for split unit compressors by H. Cao et al. (2024), vibration suppression control in rotary compressors by Y. Notohara et al. (2021), and friction excitation in rotary compressors by Y. Hu et al. (2022). Despite the extensive literature on compressors, there is a paucity of studies focused specifically on the condition monitoring of an AAC compressor.

Condition monitoring includes the assessment of machinery via vibration signals (Bai et al. 2023), acoustic emissions (García Márquez, Bernalte Sánchez & Segovia Ramírez 2022), temperature measurements (Mawson & Hughes 2020), voltage readings (Thekkuden & Mourad 2019), and oil analysis data (Hogenberk et al. 2023). All sensor data were collected and analyzed statistically based on the machine's characteristics. This preventive measure or predictive maintenance would mitigate costly maintenance expenses, significant faults, reduced efficiency, diminished service reliability, and downtime (Baboli et al. 2021). Nonetheless, there is a particular expense associated with installing the requisite sensors for

machine monitoring. Over the past 10 years, numerous studies have established the vibration pattern for machine condition monitoring (Gonzalez et al. 2020; Satar et al. 2021; Wu et al. 2022; Ye, Ji & Han 2020; Zhang et al. 2022). Statistical techniques were used to examine the pattern, such as mean, median, mode, standard deviation, variance, root mean square (RMS), skewness, kurtosis, and regression analysis. Kurtosis in statistical analysis effectively quantifies the peakedness of a distribution (Jammalamadaka et al. 2021). The integrated kurtosis-based algorithm for Z-filter (I-kaz), grounded in the time domain, was employed to monitor machine vibration patterns, material qualities, and sound recognition. The latest investigation was on bearing faulty conditions (Othman et al. 2023). Subsequently, the Integrated-Kurtosis-Frequency utilizing Z-filter (Z-freq) is a statistical analysis grounded in the frequency domain, developed by N. Ngatiman et al. (2021), for monitoring spark plug failure detection taking piezo-film as the input sensor. The researcher mentioned the potential use of other sensors, such as accelerometers and microphones, for future research.

Despite intensive vibration analyses for fault detection, no prior research has quantitatively linked multi-axis vibration to compressor oil level adequacy. The novelty of this study lies in introducing the Z-freq 3D statistical framework to the compressive oil diagnosis problem. Z-freq 3D represents three-dimensional data of integrated kurtosis frequency derived from a frequency domain signal. It is an enhancement of Z-freq analysis. This approach culminates in a new control chart called as Z-Chart. It is the first to correlate triaxial vibration features with specific oil volumes. By filling the stated knowledge gap, the study provides unique insight into vibration signal interpretation for lubrication health. The findings are significant for the field of predictive maintenance, as they advance the state-of-the-art in statistical modelling of machine health. The Gauss Amp model-derived coefficient (b/a) from Z-freq 3D analysis can serve as a robust predictor of oil sufficiency. This study is founded on the analysis of vibration signals from a belt-driven car air conditioning compressor, considering different compressor speeds and oil quantities. The Z-freq 3D will reveal a distinctive vibration pattern for optimal oil fill, distinctly different from patterns underfilled and overfilled conditions. This document is structured as follows: The Methodology section delineates the formulation behind Z-freq 3D statistical analysis and the experimental configuration. The result and discussion section delineates the observations obtained from the experiment to

corroborate the theory. A novel Z-Chart for forecasting the inadequacy of oil in a belt-driven automobile AC compressor was introduced. Conclusions are delineated in the last section to conclude the outcome of this research.

METHODOLOGY

STATISTICAL ANALYSIS USING Z-FREQ 3D

This study employed the Z_{3D}^f approach to analyze the signals from the compressor. The initial data was gathered with a three-axis accelerometer: horizontal, vertical, and axial. Frequency data was derived from the raw data using the Fast Fourier Transform (FFT). The kurtosis for each dataset was computed using Equation 1. The fourth-order moment of kurtosis was computed due to its impact on the data signal's spikiness (Cacuci & Fang 2024). Where K_{a_x} , K_{a_y} and K_{a_z} represent the kurtosis of the accelerometer along different axes, and S_{a_x} , S_{a_y} and S_{a_z} denote the standard deviations, respectively. Variables $x_i^{a_x}$, $x_i^{a_y}$ and $x_i^{a_z}$ represent data at the i th sample of frequency, while μ_{a_x} , μ_{a_y} and μ_{a_z} denote the means of each data set, with n indicating the number of samples.

Subsequent computations were conducted utilizing the formula Z_{3D}^f as delineated in equation 2. This entails the multiplication of K_{a_x} , K_{a_y} and K_{a_z} with S_{a_x} , S_{a_y} and S_{a_z} , respectively. The precision of the data was enhanced with the application of the Z-Notch filtering technique (Z-NF) which proposed by Nuawi et al. (2008). The Z-NF will eliminate background noise from the engine, belts, and other moving components associated with the A/C compressor. The equation for Z-NF is shown in Equation 3.

$$\begin{aligned} K_{a_x} &= \frac{1}{nS_{a_x}^4} \sum_{i=1}^n (x_i^{a_x} - \mu_{a_x})^4; \\ K_{a_y} &= \frac{1}{nS_{a_y}^4} \sum_{i=1}^n (x_i^{a_y} - \mu_{a_y})^4; \end{aligned} \quad (1)$$

$$\begin{aligned} K_{a_z} &= \frac{1}{nS_{a_z}^4} \sum_{i=1}^n (x_i^{a_z} - \mu_{a_z})^4 \\ Z_{3D}^f &= \frac{1}{n} \sqrt{K_{a_x}S_{a_x}^4 + K_{a_y}S_{a_y}^4 + K_{a_z}S_{a_z}^4} \end{aligned} \quad (2)$$

$$\begin{aligned} \text{Filtered frequency (data)} &= \text{Wet Run (data + noise)} - \\ \text{Dry Run (noise)} & \end{aligned} \quad (3)$$

EXPERIMENT SETUP

The experiment was set up using a compact car 1.5cc with A/C compressor model XI447260-9990. The compressor was charged with 320g of refrigerant type R134a with oil quantities ranging from 40 ml to 120 ml in 20 ml increments for each condition. The car was stationed beneath a hangar with an ambient temperature of 25 degrees Celsius. The compressor speed varied from 1300 rpm to 2700 rpm. For each parameter, three sets of data of 5 seconds were collected and analyzed.

The vibration sensor employed was the MEMS triaxial accelerometer from the Phantom ATEX model, operating at a sampling frequency of 3200 Hz. It transmits the data wirelessly to the Phantom Cloud Storage via Phantom Gateway and Internet Router. All vibration signals were downloaded to DigivibeMX Phantom software. Figure 1 illustrates the comprehensive configuration of the connection for data collecting. The phantom ATEX was attached to one end of the compressor to record the triaxial reading, as illustrated in Figure 2.

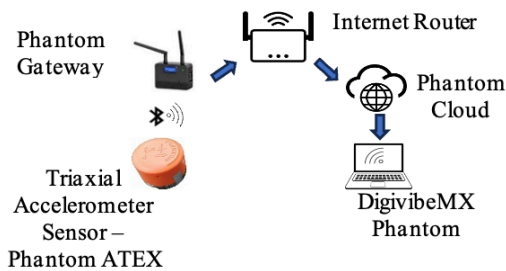


FIGURE 1. Phantom ATEX configuration for data collection

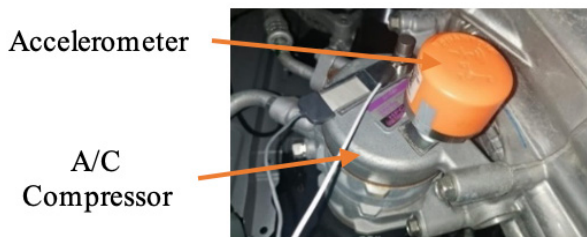


FIGURE 2. Experiment Setup

Figure 3 below illustrates the workflow for A/C diagnostics using Z_{3D}^f . The calculated value of Z_{3D}^f coefficient was subsequently simulated in three-dimensional graphical form. A graph of Z_{3D}^f versus oil quantity was then created to illustrate its correlation. The curve fitting function was used to generate the graph and producing an equation for each oil quantity. The Z-Chart was subsequently

constructed using the 'b/a' coefficient in relation to the quantity of oil.

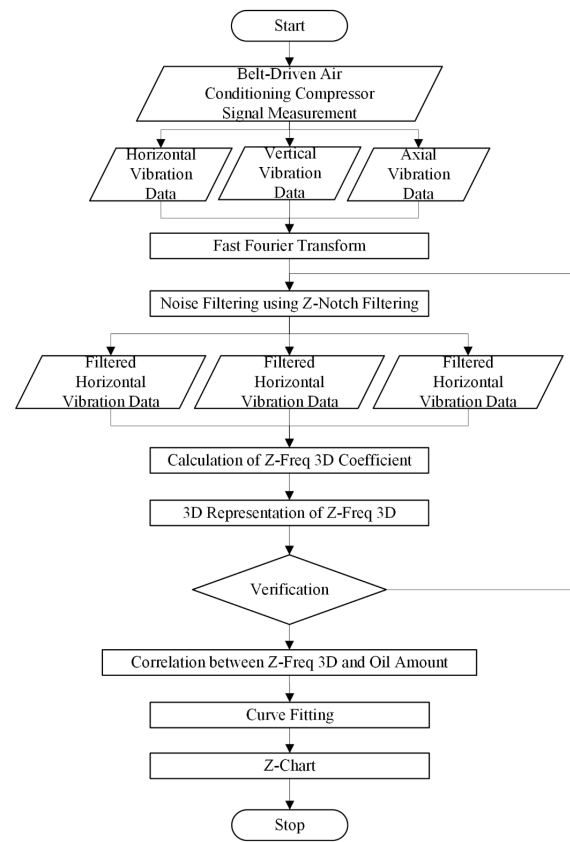


FIGURE 3. A/C compressor fault diagnostic process flow using Z-freq 3D

RESULTS AND DISCUSSION

Z-FREQ ANALYSIS

Table 1 displays the time domain graphs of low, medium and maximum quantities of AAC compressor oil at a compressor speed of 2100 rpm. The acceleration signal across all three axes exhibits a significantly higher amplitude during the A/C on condition compared to the A/C off state. This signifies that the compressor is under strain, compressing the refrigerant, hence generating friction and amplifying the vibration (Borzea et al. 2021). The axial direction exhibits more sensitivity to the load, evidenced by a more pronounced amplitude variation. This is attributable to the axial orientation of the compressor piston (Zhang et al. 2022). All time-domain graphs were subsequently transformed into frequency-domain graphs using the Fast Fourier Transform (FFT) as shown in Table 2. Consequently, this signifies that the residual frequencies are essential frequencies for compressor vibration.

Figure 4 below illustrates the variation of the Z_{3D}^f graph at different oil quantities during operation at 2100 rpm for 40 ml, 80 ml, and 120 ml. The scattering point trends are analogous across the three situations, indicating that they measure the same compressor type. The pattern of oil deficiency and oil overfill is distinctly observable using the Z_{3D}^f coefficient. The values for Z_{3D}^f are $3.58e^{-3}$ and $3.22e^{-3}$ for 40 ml and 120 ml respectively, which are

greater than $1.58e^{-3}$ for 80 ml. A larger Z_{3D}^f coefficient signifies an elevated level of vibration. A larger Z_{3D}^f coefficient signifies an elevated level of vibration. The image additionally illustrates that the dots are more dispersed in all directions, indicating greater vibration amplitudes in the A/C under the specified condition compared to 80ml.

TABLE 1. Time domain for AAC compressor at 2100rpm

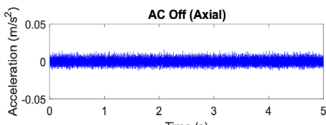
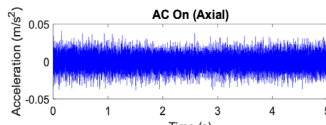
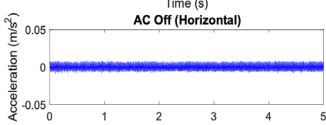
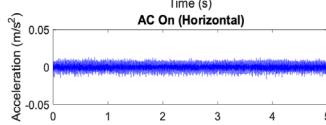
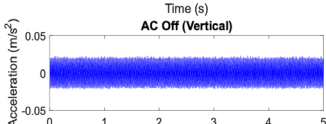
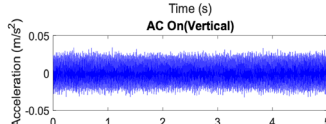
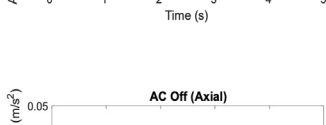
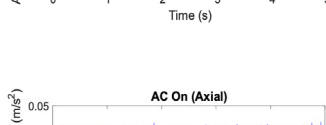
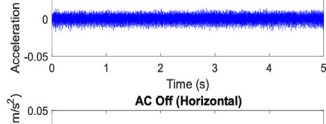
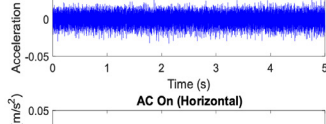
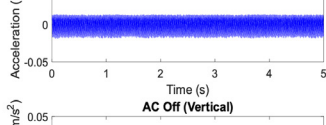
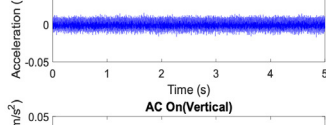
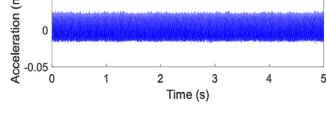
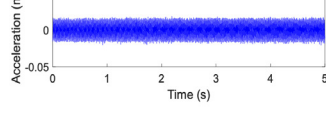
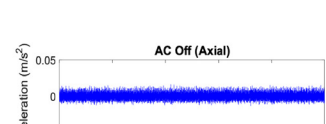
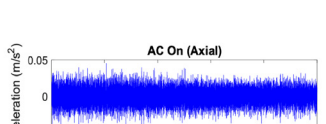
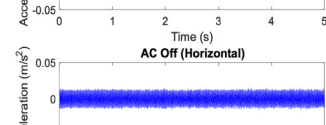
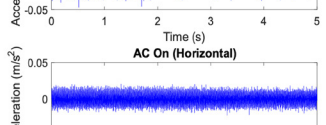
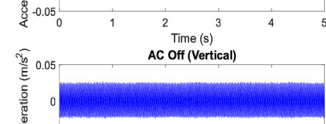
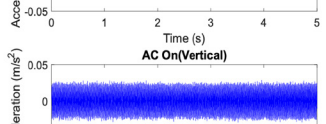
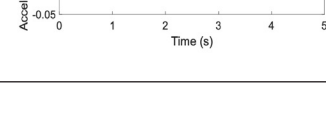
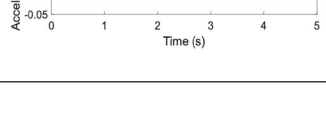




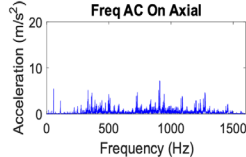
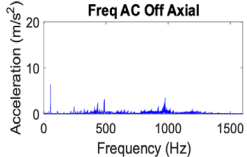
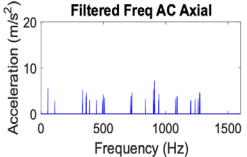
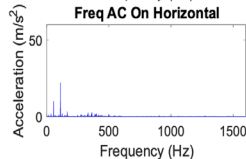
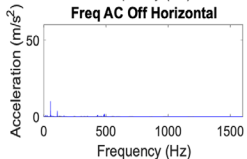
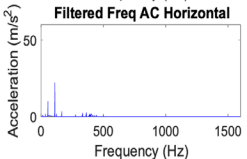
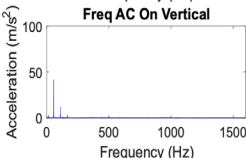
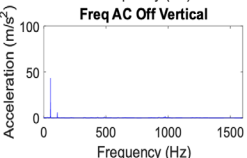
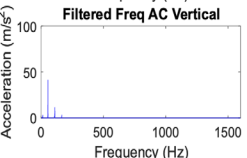
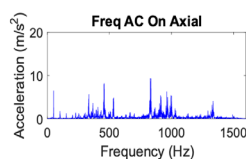
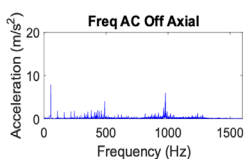
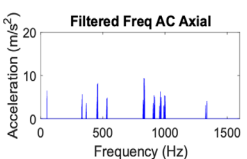
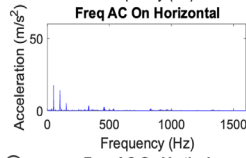
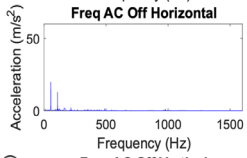
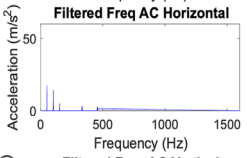
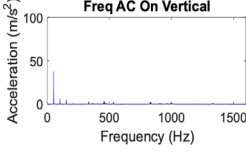
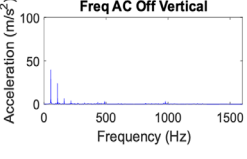
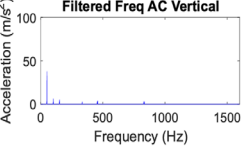
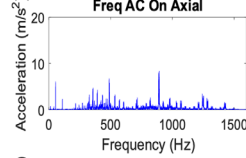
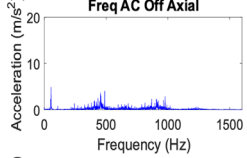
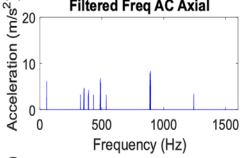
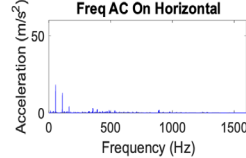
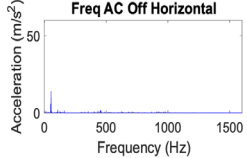
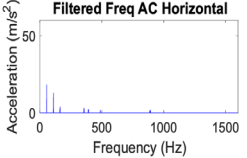
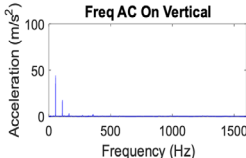
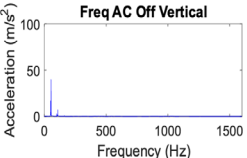
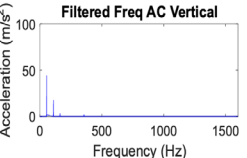
Compressor Oil Amount	Time Domain Graph				
40ml					
					
					
					
					
					
80ml					
					
					
					
					
					
120ml					

TABLE 2. Frequency domain during A/C on, A/C off and Filtered Frequency Domain at 2100 rpm

Compressor Oil Amount	Graph		
	(a)	(b)	(c)
40ml			
			
			
80ml			
			
			
120ml			
			
			

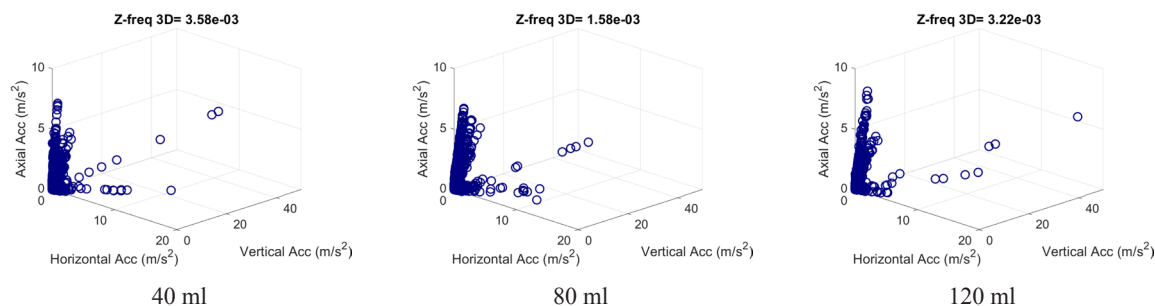


FIGURE 4. Z-freq 3D graph for 40ml, 80ml and 120ml

COMPARISON BETWEEN AVERAGE MEASURED RMS AND Z-FREQ 3D

Table 3 presents the value of Z_{3D}^f and average measured RMS value (ARMS) for various quantities of compressor oil and at varied compressor speeds ranging from 1300 rpm to 2700 rpm. The value of Z_{3D}^f and ARMS rise proportionally with the increase of compressor speed. Increasing the speed would definitely increase the movement of the piston inside the compressor and increase the vibration of the compressor. A graph of ARMS versus Z_{3D}^f was plotted to examine the correlation between the two variables. The quadratic polynomial regression curve

fitting approach was employed to illustrate the relationship between ARMS and Z_{3D}^f . The parabolic equation is $ARMS = -0.13132(Z_{3D}^f)^2 + 2.79495(Z_{3D}^f)$. The correlation between ARMS and Z_{3D}^f is exceptionally good, with an R-squared value of 94%, as illustrated in Figure 5(a).

Utilizing the aforementioned mathematical model, the ARMS value for the identical AAC compressor model could be easily predicted. Figure 5(b) illustrates the scatter diagram of predicted versus measured values for all 30 datasets. Most of the points roughly correspond to the linear regression line. The correlation between predicted and measured values is extreme, with an R^2 value of 94%. Consequently, Z-freq 3D serves as an appropriate substitute for monitoring the oil level in AAC compressors.

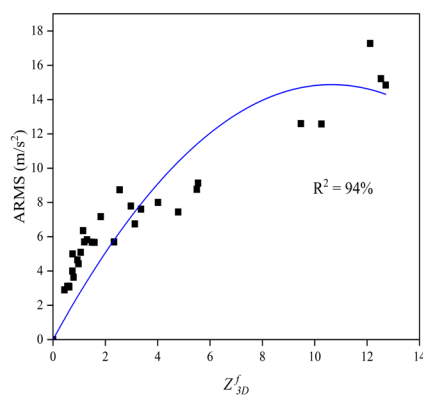
TABLE 3. Experiments on Air Conditioning Compressor Oil at 320g R4310

Experiment No.	Compressor Oil Amount (ml)	Compressor Speed (rpm)	Average Z_{3D}^f	ARMS (m/s ²)
Exp.1	40	1300	0.786	3.640
		1400	1.057	5.095
		1600	1.197	5.698
		2100	3.361	7.611
		2400	5.494	8.765
		2700	12.525	15.221
Exp.2	60	1300	0.437	3.111
		1400	0.741	4.206
		1600	1.583	5.961
		2100	2.330	6.152
		2400	4.011	8.387
		2700	10.254	12.600

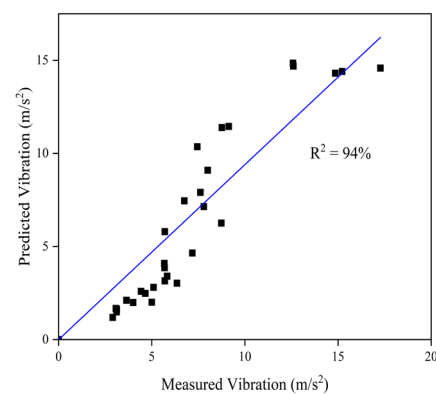
continue ...

... cont.

Exp.3	80	1300	0.602	3.121
		1400	0.930	4.654
		1600	1.298	5.822
		2100	1.820	7.176
		2400	2.544	8.737
		2700	9.472	12.600
Exp.4	100	1300	0.618	3.253
		1400	0.972	4.625
		1600	1.485	6.074
		2100	3.127	7.094
		2400	4.783	7.821
		2700	12.119	14.849
Exp.5	120	1300	0.548	3.111
		1400	0.745	5.001
		1600	1.147	6.354
		2100	2.972	7.792
		2400	5.540	9.133
		2700	12.119	17.274



(a)



(b)

FIGURE 5. Correlation between ARMS versus Z_{3D}^f and Predicted Vibration versus Measured Vibration

Z-CHART FOR PREDICTING COMPRESSOR OIL DEFICIENCY

Figure 6 illustrates the exponential fit graph of Z_{3D}^f versus compressor speed for five distinct oil quantities. Z_{3D}^f index

escalates with an increase in compressor speed is increased. The exponential fit of Z_{3D}^f successfully distinguishes among the five varying oil quantities. The lowest curve of the graph, depicted by the blue line, represents the 80ml compressor oil followed by 60 ml (red line), 100 ml (green

line), 120 ml (purple line) and 40 ml (black line). Consequently, five different equations relating Z_{3D}^f to compressor speed was derived from an exponential equation with the general form is $Z_{3D}^f = a \times b^{rpm}$. Five distinct values of the coefficient 'a' and 'b' were produced, as illustrated in Table 4 below. The coefficient 'b/a' was calculated and selected for plotting again the refrigerant oil because of its strong sensitivity to the oil volume, as illustrated in Figure 5. It creates a bell-shaped graph, called a Z-Chart, with a coefficient of determination of 99%. The optimal point occurs at 80 ml, where the 'b/a' coefficient attains its maximum value of 864.94. This indicates the belt-driven compressor of the AAC system achieves its optimal vibration characteristic at this oil level. The 'b/a' coefficient decreased and fell below 85.2 when the oil level was reduced to 60 ml or 40 ml, or increased to 100 ml or 120 ml. Both inefficient and excessive oil volumes lead to

suboptimal performance of the compressor. The graph equation is $y = 45.432 + 819.507e^{-\frac{(x-80)^2}{128}}$ which is derived from the Gauss Amp model. The oil quantity in milliliters can be readily determined by calculating the ratio of 'b/a' for compressor model XI447260-9990.

The result of this study has clear implications for real-world applications in automotive maintenance. In particular, the Z-Chart diagnostic approach can be translated into practical tools and protocols in the scheduled service routines. A service technician could use a handheld triaxial accelerometer to assess compressor vibration during routine check-ups quickly. If the measured b/a ratio deviated from the range around the peak, it would signal oil inadequacy. This enables the technician to top up or remove oil to reach the optimal fill before the compressor suffers damage.

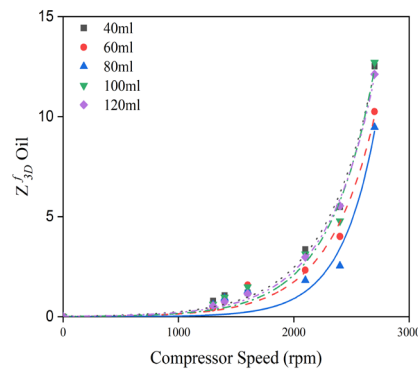


FIGURE 6. Z_{3D}^f Oil versus Compressor Speed (rpm)

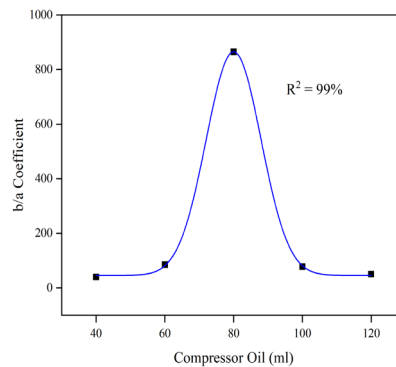


FIGURE 7. Z Chart of b coefficient versus Refrigerant Oil

TABLE 4. 'a' and 'b' coefficient on Varying Compressor Oil Amount

		Compressor Oil (ml)				
		40	60	80	100	120
Coefficient	a	0.02500	0.01177	0.00116	0.01290	0.01974
	b	1.00230	1.00250	1.00333	1.00255	1.00238
	b/a	40.09200	85.17417	864.93966	77.71705	50.77913

CONCLUSION

This research successfully demonstrated a novel vibration-based diagnostic for an automotive compressor oil level. The findings indicated that the 'b/a' coefficient derived from the Z-freq 3D exponential fit curve model serves as a highly sensitive indicator of oil adequacy. Compressor operating at the optimal oil fill (80 ml) exhibited a distinct vibration signature that was statistically differentiated from both under-filled and over-filled cases. The ability of the Gauss Amp model to fit a bell curve to the b/a versus oil volume with 99% of R^2 is particularly noteworthy, as it underscores the strong, quantifiable relationship between lubricant and vibration behavior.

The novelty of this work lies in integrating multi-axis frequency domain statistical features (kurtosis-based) with a Gaussian modal approach to create a practical diagnostic chart called the Z-Chart. This is the first application of Z-freq 3D in the context of lubrication monitoring, marking a significant advancement beyond conventional vibration analysis techniques. Z-Chart can be directly used to guide predictive maintenance decisions, allowing practitioners to identify and correct suboptimal oil levels. This enhances compressor reliability, improves efficiency, and reduces maintenance costs and downtime for automotive HVAC systems.

Ultimately, this study fills a crucial gap in the field of automotive maintenance engineering by quantifying the impact of oil quantity on vibration and providing a clear criterion for optimal lubrication. The insight gained here not only paves the way for smarter vehicle health monitoring systems by integrating with real-time IoT-enabled systems but also sets a precedent for applying this advanced statistical model to other condition monitoring. The approach and result presented can serve as a reference point for future researchers and engineers aiming to ensure mechanical systems operate at peak performance through data-driven maintenance strategies.

ACKNOWLEDGEMENT

The author wishes to express gratitude to Universiti Kebangsaan Malaysia (UKM) and Universiti Teknikal Malaysia Melaka (UTeM) for their support of this research.

DECLARATION OF COMPETING INTEREST

None

REFERENCES

- Al-Zahrani, A. 2024. Investigating new environmentally friendly zeotropic refrigerants as possible replacements for Carbon Dioxide (CO₂) in car air conditioners. *Sustainability* 16(1).
- Alahmer, A. & Ghoniem, R.M. 2023. Improving automotive air conditioning system performance using composite nano-lubricants and fuzzy modeling optimization. *Sustainability* 15(12).
- Aziz, M.S.A., Mazlan, A.Z.A., Satar, M.H.A., Paiman, M.A.R., Ghapar, M.Z.A. & Abd Ghapar, M.Z. 2022. Attenuation of humming-type noise and vibration in vehicle HVAC system using a tuneable dynamic vibration absorber. *Archives of Acoustics* 47(3): 331–342.
- Baboli, P.T., Babazadeh, D., Raeiszadeh, A., Horodyvskyy, S. & Koprek, I. 2021. Optimal temperature-based condition monitoring system for wind turbines. *Infrastructures* 6(4).
- Bai, W., Zhou, X., Wang, Y., Zeng, Q., Zhan, S., Hua, X. & Bao, G. 2023. Vibration analysis of the electric drive system with inter-turn short-circuit and gear spalling faults. *Journal of Vibration Engineering & Technologies* 11(8): 3595–3605.
- Borzea, C., Petrescu, V., Vlăduță, I., Roman, M. & Badea, G. 2021. Potential of twin-screw compressor as vibration source for energy harvesting applications. *Actualități Și Perspective În Domeniul Mașinilor Electrice (Electric Machines, Materials and Drives - Present and Trends)* 2021(1): 1–6.
- Cacuci, D.G. & Fang, R. 2024. Review of fourth-order predictive modeling and illustrative application to a nuclear reactor benchmark. I. typical high-order sensitivity and uncertainty analysis. *Energies* 17(16).
- Cao, H.-F., Yang, C.-J., Ma, R.-L., Ni, S.-W., Song, Z.-K., Wang, X., Chen, Y.-X. & Jiang, C.-X. 2024. An investigation of the acoustic enclosure of an air conditioning compressor using response surface analysis and topological rigidity optimization. *Shock And Vibration* 2024.
- Chen, X., Liang, K., Li, Z., Zhao, Y., Xu, J. & Jiang, H. 2020. Experimental assessment of alternative low global warming potential refrigerants for automotive air conditioners application. *Case Studies In Thermal Engineering* 22(August): 100800.
- Duan, H., Ming, X., Zhang, X.-B., Sterner, T. & Wang, S. 2023. China's adaptive response to climate change through air-conditioning. *Iscience* 26(3).
- Fan, P., Ma, X., Chen, Y., Yuan, T. & Liu, T. 2022. Optimization of the automotive air conditioning system using radial basis function neural network. *Thermal Science* 26(4): 3477–3489.
- Fukagawa, K., Kurazumi, Y., Aruninta, A., Yamato, Y. & Hayashi, Y. 2023. Effect of visual stimuli on human thermal sensation of short term residents in

- an outdoor campus landscape in a tropical climate. *International Journal of Geomate* 25(108): 89–96.
- Gajanayake, S., Bandara, S. & Sugathapala, T. 2023. A novel approach to estimate power demand of auxiliary engine loads of light duty vehicles. *Frontiers in Mechanical Engineering-Switzerland* 8.
- García Márquez, F.P., Bernalte Sánchez, P.J. & Segovia Ramírez, I. 2022. Acoustic inspection system with unmanned aerial vehicles for wind turbines structure health monitoring. *Structural Health Monitoring* 21(2): 485–500.
- Golofit-Szymczak, M., Stobnicka-Kupiec, A. & Gorny, R.L. 2019. Impact of air-conditioning system disinfection on microbial contamination of passenger cars. *Air Quality Atmosphere and Health* 12(9): 1127–1135.
- Gonzalez, J., Delgado, L., Velarde-Suarez, S., Fernandez-Oro, J.M., Arguelles Diaz, K.M., Rodriguez, D. & Mendez, D. 2020. Experimental study of the unsteady vibration signature for a Sirocco fan unit. *Journal Of Low Frequency Noise Vibration and Active Control* 39(1): 129–148.
- Hamisa, A.H., Azmi, W.H., Ismail, M.F., Rahim, R.A. & Ali, H.M. 2023. Tribology performance of polyol-ester based TiO_2 , SiO_2 , and their hybrid nanolubricants. *Lubricants* 11(1).
- Harvey, G., Bain-Donohue, S. & Dewi, S.P. 2024. The impact of extreme heat on older regional and rural Australians: A systematic review. *Australian Journal of Rural Health* 32(2): 216–226.
- He, Z., Ji, L. & Xing, Z. 2020. Experimental investigation on the DLC film coating technology in scroll compressors of automobile air conditioning. *Energies* 13(19).
- Hogenberk, F., Osara, J.A., van den Ende, D. & Lugt, P.M. 2023. On the evolution of oil-separation properties of lubricating greases under shear degradation. *Tribology International* 179(October 2022): 108154.
- Hu, Y., Zhang, R., Zhang, J., Song, Q. & Chen, G. 2022. Friction-excited oscillation of air conditioner rotary compressors: measurements and numerical simulations. *Lubricants* 10(4).
- Jammalamadaka, S.R., Taufer, E. & Terdik, G.H. 2021. On multivariate skewness and kurtosis. *Sankhya: The Indian Journal of Statistics* 83(2): 607–644.
- Kumar, S.R., Ali, M.S.W., Pandian, C.K.A., Muralidharan, V., Ravi Kumar, S., Syed Wahid Ali, M., Pandian, C.K.A. & Muralidharan, V. 2024. Condition monitoring of electric vehicle motor testing machine's Vital components using bagged trees and quadratic SVM: a comparative study. *Engineering Research Express* 6(2): 025531.
- Mawson, V.J. & Hughes, B.R. 2020. Deep learning techniques for energy forecasting and condition monitoring in the manufacturing sector. *Energy And Buildings* 217.
- Notohara, Y., Li, D., Iwaji, Y., Tamura, M. & Tsukii, K. 2021. Study on vibration suppression control for rotary compressor. *IEEJ Journal of Industry Applications* 10(4): 481–486.
- Nuawi, M.Z., Lamin, F., Nor, M.J.M., Jamaluddin, N. & Abdullah, S. 2008. The noise cancelling technique using z-filter on machining signal(January): 274–279.
- Othman, A., Hamid, H., Ahmad, M.A.F. & Nuawi, M.Z. 2023. Comparison study on pinch-hitting vibration signal analysis for automotive bearing: I-KazTM and I-Kaz 3D. *International Journal of Integrated Engineering* 15(5): 253–262.
- Parent, T., Defoe, J.J. & Rahimi, A. 2023. Nonlinear modeling of an automotive air conditioning system considering active grille shutters. *Modelling* 4(1): 70–86.
- Patel, B. & Parekh, A. 2024. Energy, exergy and entropy analysis with R1234yf as an alternate refrigerant to R134a of automobile air conditioning system. *Journal of Thermal Engineering* 10(1): 101–114.
- Randazzo, T., Pavanello, F. & De Cian, E. 2023. Adaptation to climate change: Air-conditioning and the role of remittances. *Journal of Environmental Economics and Management* 120.
- Saadoon, Y.G. & Aljubury, I.M. 2019. Experimental analysis of mobile air conditioning system using R513a as alternative refrigerants to R134a. *Journal of Mechanics of Continua And Mathematical Sciences* 14(6): 450–469.
- Safril, Azmi, W.H., Sharif, M.Z. & Zawawi, N.N.M.M. 2024. The tribology evaluation on a four-ball tribometer lubricated by Al2O3/PAG nanolubricants. *International Journal of Automotive and Mechanical Engineering* 21(1): 11055–11063.
- Sanzana, M.R., Maul, T., Wong, J.Y., Abdulrazic, M.O.M. & Yip, C.-C. 2022. Application of deep learning in facility management and maintenance for heating, ventilation, and air conditioning. *Automation in Construction* 141(June): 104445.
- Satar, M.H.A., Mazlan, A.Z.A., Hamdan, M.H., Isa, M.S.M., Paiman, M.A.R. & Ghapar, M.Z.A. 2021a. A lab-scale HVAC hissing-type noise and vibration characterization with vehicle system validation. *Archives of Acoustics* 46(2): 365–373.
- Satar, M.H.A., Mazlan, A.Z.A., Hamdan, M.H., IsA, M.S.M., Paiman, M.A.R., Ghapar, M.Z.A. & Abd Ghapar, M.Z. 2021b. Experimental validation of the HVAC humming-type noise and vibration in model and vehicle system levels. *Archives of Acoustics* 46(2): 375–385.
- Schaut, S. & Sawodny, O. 2020. Thermal management for the cabin of a battery electric vehicle considering passengers' comfort. *IEEE Transactions on Control Systems Technology* 28(4): 1476–1492.

- Shalgar, S. & Bindu, R. 2022. Design and development of a novel multichannel data acquisition system using labview for an automobile air conditioning application. *Journal of Thermal Engineering* 8(1): 14–28.
- Thekkuden, D.T. & Mourad, A.H.I. 2019. Investigation of feed-forward back propagation ANN using voltage signals for the early prediction of the welding defect. *SN Applied Sciences* 1(12): 1–17.
- Vasta, S. 2023. Adsorption air-conditioning for automotive applications: A critical review. *Energies* 16(14).
- Wu, J.-D., Ke, J.-Y., Shih, F.-Y. & Shyr, W.-J. 2022. Fault diagnosis for vehicle air conditioning blower using deep learning neural network. *Journal of Low Frequency Noise Vibration and Active Control* 41(3): 910–925.
- Xiao, W., Shi, J. & Chen, H. 2023. Research on optimal design of vibration reduction of centrifugal air conditioning chiller based on particle damping. *Journal of Theoretical and Applied Mechanics* (2004): 189–201.
- Ye, K., Ji, J. & Han, S. 2020. Semi-active noise control for a hermetic digital scroll compressor. *Journal of Low Frequency Noise Vibration and Active Control* 39(4): 1204–1215.
- Zawawi, N.N.M., Hamisa, A.H., Azmi, W.H., Hendrawati, T.Y. & Safril, S. 2023. Performance of hybrid electric vehicle air-conditioning using SiO₂/POE nanolubricant. *Case Studies in Thermal Engineering* 52(August): 103717.
- Zawawi, N.N.M.M., Azmi, W.H., Hamisa, A.H., Hendrawati, T.Y. & Aminullah, A.R.M.M. 2024. Experimental investigation of air-conditioning electrical compressor using binary TiO₂-SiO₂ polyol-ester nanolubricants. *Case Studies in Thermal Engineering* 54(February): 104045.
- Zhang, H., Cao, S., Li, P. & Han, Q. 2022a. Self-excited vibration analysis of gear-bearing system with multipoint mesh and variable bearing dynamic coefficients. *Shock and Vibration* 2022.
- Zhang, R., Zhang, J., Song, Q. & Chen, G. 2022b. Study on the extraction method of the friction-induced vibration signal of rotary compressors. *Journal of Vibroengineering* 24(7): 1213–1225.